Bayesian Optimization of Light Grating for High Performance Single-Photon Avalanche Diodes

1st Jérémy Grebot
STMicroelectronics, INRIA, Silvaco,
Crolles, France
jeremy.grebot@silvaco.com

2nd Rémi Helleboid
STMicroelectronics
Crolles, France

3rd Gabriel Mugny
STMicroelectronics
Grenoble, France

4th Isobel Nicholson
STMicroelectronics
Edinburgh, United-Kingdom

5th Louis-Henri Fernandez Mouron
STMicroelectronics
Crolles, France

6th Stéphane Lanteri
UCA, Inria, CNRS, LJAD, Inria Research Center,
Sophia-Antipolis, France

7th Denis Rideau
STMicroelectronics
Crolles, France

***Abstract*—Bayesian optimization is used to investigate the optimal grating parameters of realistic SPADs, enhancing high absorption by positioning a resonance exactly at 940 nm. Bayesian optimization allows us to find optimal parameters while minimizing the numerical cost required.**

***Index Terms*—Bayesian optimization, SPADs, diffractive grating, resonance, RCWA, optical, absorption**

I. Introduction

CMOS image sensors (CIS) for the near infrared range (NIR) sensing are currently used in a great number of smartphones, laptops, and digital cameras, but also in various areas such as biological inspection, Time-of-Flight (ToF) and fiber optic communication [1]. NIR light, in particular the wavelength of 940 nm, is mostly used because of its invisibility to the human eye, allowing constant illuminations required, for example, by distance measurement or facial recognition. However, CIS tends to show low efficiency at such wavelengths mainly because silicon, due to its indirect bandgap value of 1.2eV, is almost transparent at this wavelength.

One way to improve NIR light absorption efficiency in CISs is to use a nanostructured pattern on top of the silicon substrate. Both plasmonic metal patterning [2], [3] yielding strong electric field enhancement by resonant coupling between photons and electrons in metal, and diffractive patterning [4] allowing to increase light propagation length and effective silicon thickness, have shown drastic increase in NIR light sensitivity of CISs. Among the various patterns used, such as the rectangular array [2], [3] or nanopillar array [5], the Inverted Pyramid Array (IPA) [6], [7] have been used in mass production [8].

The design of such nanoscale patterning schemes heavily relies on numerical modeling and, in most cases, multi-parametric simulations are performed to obtain an exploitable picture of the role of each geometric parameter. Depending on the complexity of the considered structures, these numerical studies can require a considerable amount of computational resources, especially in the general three-dimensional setting. An alternative and attractive approach is to resort to a numerical optimization approach for discovering optimal sets of geometrical parameters. Although such numerical optimization strategies have been extensively considered in the recent years for metamaterial design and metasurfaces (see in particular [9]), their development for nanostructured CMOS image sensors seems to be less remarkable.

In this work, we introduce an inverse design approach that combines optical solvers for the numerical characterization of light absorption in a nanostructured CMOS image sensor, with a statistical learning-based global optimization method, for goal-oriented discovery of the optimal patterning parameters. Realistic 2D SPAD with side DTI to isolate pixels can reach up to an absorption of 80% at 940 nm.

II. Problem statement

The problem of improving the performance of diffractive grating arrays has been widely studied in literature [2], [3], [5], [8], [10]. Some interesting contributions focusing on the grating itself can provide a physical intuition of the transmitting diffractive orders or on the optimization and the increase of the effective light path length within the pixel [2]. However, in a "resonant-chamber-like pixel" exhibiting sidewall Deep Trenches Isolation (DTI), such an approach can fail to predict resonances that may occur in the whole pixel. We would like to study and optimize the resonances, resulting from a diffraction grating in a SPAD pixel with DTIs. We consider pixels operating in a monochromatic mode, including the study of geometrical parameters and their interactions. A resonance is here defined as a peak in the absorption profile. Increasing the light absorption, at 940 nm, in a pixel, may be equivalent to positioning a resonance exactly at 940 nm. The maximization of the light absorption at 940 nm is performed with Bayesian optimization, also referred to as Efficient Global Optimization (EGO) [11]. The optical absorption for each design is calculated with a 2D/3D in-house rigorous coupled wave analysis (RCWA) solver [12]. Fig. 1 shows the output

of the optical solver, from which the objective function is computed.

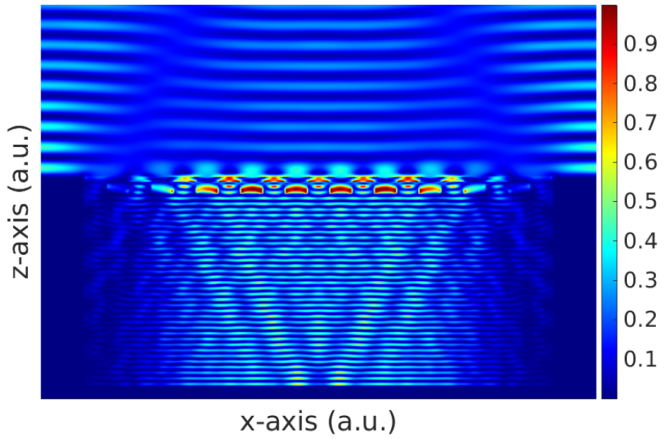

Fig. 1. Map of the electric field norm for the optimized structure at λ = 940 nm. The grating enables an important diffraction of the light. In particular, the first diffraction order is visible through the angular path of the light within the Silicon. The null electric field outside the active silicon shows that DTIs successfully confine the light. Using the Ohmic losses formula, the absorption within the active region is obtained by integrating the norm of the electric field over the active region:
$\mathrm{A}(\lambda) = \frac{\varepsilon_0 \lambda}{2} \int \mathrm{Im}(\varepsilon_{\mathrm{Si}}) |\mathbf{E}|^2$.

Relevant SPAD geometrical parameters to be optimized are shown in Figs. 2 and 3. They include the grating ones but also the side DTIs position, L_{DTI}, and thickness, $L_{rl,DTI}$, as well as the Si thickness L_{epi}.

For three-dimensional structure, circular 2D grating, shown on Fig. 4, has been chosen as an example of 2D expansion of the 1D grating, shown in Fig. 3, on both x and y-axis.

As it can be seen in Fig. 5 (resp. Fig. 6), the absorption as a function of the structuration pattern depth L_{depth} (resp. the structuration pitch L_{pitch}), exhibits multiple resonances. Findind optimal parameters aims to combine these resonances. This greatly justifies the relevance of a global optimization approach and prevents any efficient use of a local optimizer, such as, for instance, conjugate gradient.

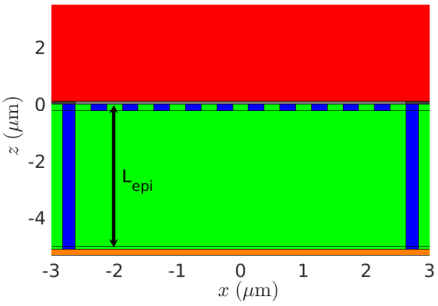

Fig. 2. 2D nanostructured SPAD, with parameters in μm: $L_{epi} = 5$, $L_{pitch} = 0.5$, $L_{depth} = 0.218$, $L_{DTI} = 0.2$, $L_{rl,DTI} = 0.5$ and nb_{pitch} = 10. Red is air, black is tungsten, grey is TA_2O_5, blue is SiO_2, green is Si and orange is Cu. The DTIs are shown as left and right blue thin rectangles. The active Si region is the central green square in between DTIs.

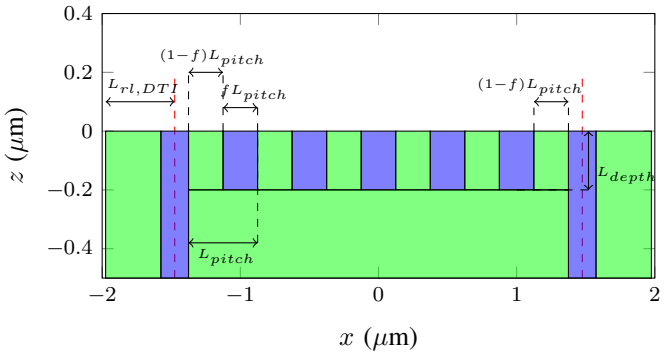

Fig. 3. Definition of L_{depth}, L_{pitch}, f, $L_{rl,DTI}$ and nb_{pitch} of the gratings. In this study, nb_{pitch} is set to 10 in 2D and 6 in 3D (only 5 are shown here for visualization purposes). Green (respectively blue) rectangles are made of Si (resp. SiO2). An extra Si pillar of length $(1-f)L_{pitch}$ is added on the right to ensure that the grating is centered, and that the distance between the trenches and the two DTI (left and right) are equal. In this example, we have: $L_{pitch} = 500$ nm, $f = 0.5$, $L_{rl,DTI} = 500$ nm and $L_{depth} = 200$ nm.

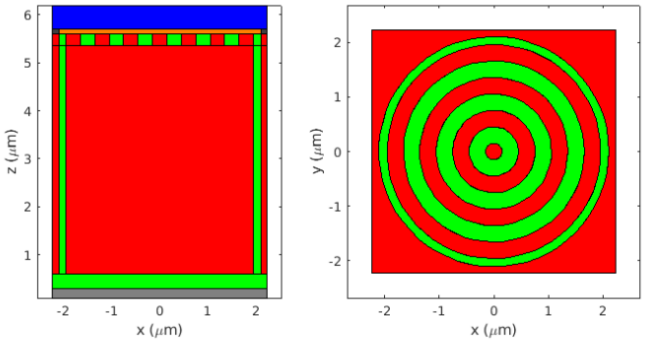

Fig. 4. 3D nanostructured SPAD, with parameters in μm: $L_{epi} = 5.5$, $L_{pitch} = 0.6$, $L_{depth} = 0.218$, $L_{DTI} = 0.2$, $L_{rl,DTI} = 0.5$ and nb_{pitch} = 6. Red is Si, green is SiO_2, blue is air, orange is TA_2O_5, grey is Cu and black tungsten. The DTIs are circular and thus adapted to the grating shapes.

III. Results

As a demonstrator of the relevance of EGO, we independently optimized two and three geometrical parameter, namely (L_{pitch}, L_{depth}) and $(L_{epi}, L_{pitch}, L_{depth})$, on 2D SPAD simulations, and we found an optimum reaching an absorption up to 80% in both cases (Fig. 7). In Fig. 8, the objective function values (the absorption at 940 nm), for each optimization iterations, are shown. The values are first increasing, then reach a plateau, showing that an optimum has been found.

Fig. 9 shows the linear sweep response on a reduced subspace (L_{pitch}, L_{depth}) and best performing parameters of the EGO optimization (when 2 parameters are considered).

Optimizing the inner Si absorption with EGO, allowed us to perform better than the 47% absorption found in [2]. Also, our methodology finds an optimum with lower numerical cost compared to a usual linear parameters sweep.

Furthermore, using the surrogate Gaussian process model allows to identify the area of coupling resonances on the

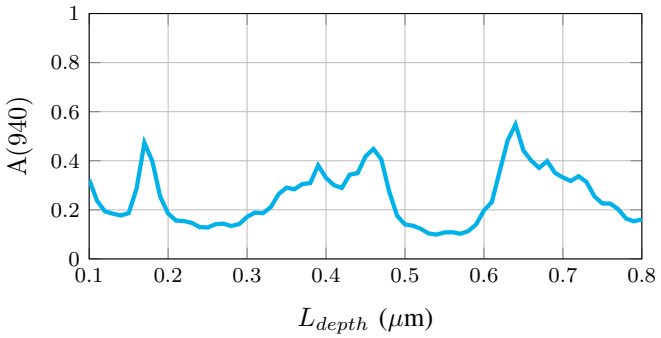

Fig. 5. RCWA 2D computation of the inner Si absorption, as a function of L_{depth} of the structure described in Figs. 2 and 3 . If not varying, we have $L_{epi} = 5$ μm, $L_{pitch} = 500$ nm and $L_{depth} = 218$ nm. A(940) denotes the inner Si absorption at 940 nm.

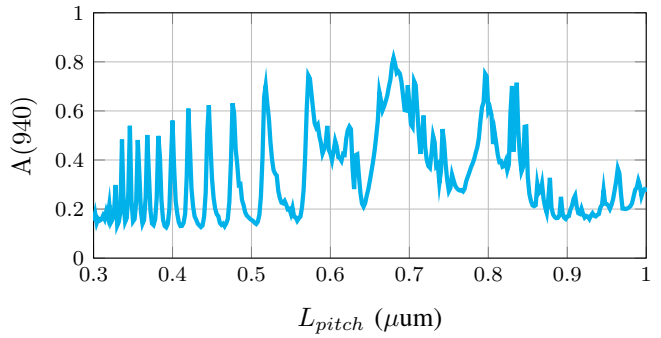

Fig. 6. RCWA 2D computation of the inner Si absorption, as a function of L_{pitch} of the structure described in Figs. 2 and 3 . If not varying, we have $L_{epi} = 5$ μm, $L_{pitch} = 500$ nm and $L_{depth} = 218$ nm. Oscillations according to the L_{pitch} variation have a higher frequency, and a higher amplitude than the ones from the L_{depth} sweep (see Fig 5).

searched parameters space. Combining the best performing designs, the prediction of the underlying Gaussian process allows us to generate more than 97 alternative designs presenting an absorption higher than 75%. This efficiency of surrogate Gaussian processes must be remembered for further studies.

Three-dimensional SPADs have been optimized on two parameters, (L_{pitch}, L_{depth}), with circular gratings, reaching an absorption up to 66%. In Fig. 10, the objective function for each optimization iterations is shown. The absorption profile of the optimal design is shown in Fig. 11. Compared to the 80% absorption obtained for the 2D SPADs, the lower absorption obtained in 3D indicates the limitation of circular gratings, which do not reproduce the resonance effect exhibited by the 1D grating optimized with 2D SPADs.

We performed the optimization of grating parameters on 2D and 3D structures. Optimization in 2D takes advantage of the low numerical cost of the simulations, which enables us both to explore a larger parameters space and to compare with the usual linear parameters sweep methodology. Typically 2D optical simulations with our in-house RCWA software last around 60 seconds, while 3D simulations last 3 hours.

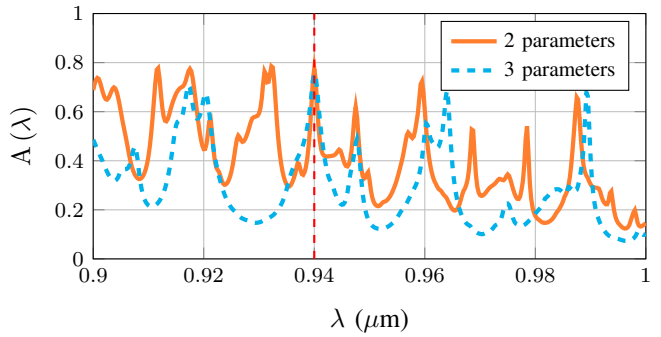

Fig. 7. Absorption profile of the best 2D designs when 3 parameters are optimized (blue curve) and when only two parameters are optimized (orange curve): optimum with parameter $(L_{epi}, L_{pitch}, L_{depth}) = (4643.3, 621.2, 275.6)$ nm^3 and $(L_{pitch}, L_{depth}) = (643.53, 356.43)$ nm^2. The two peaks at 940 nm show that the Bayesian optimizer successfully positioned a resonance at the desired wavelength. For simplicity, only TM polarized incident light is considered here.

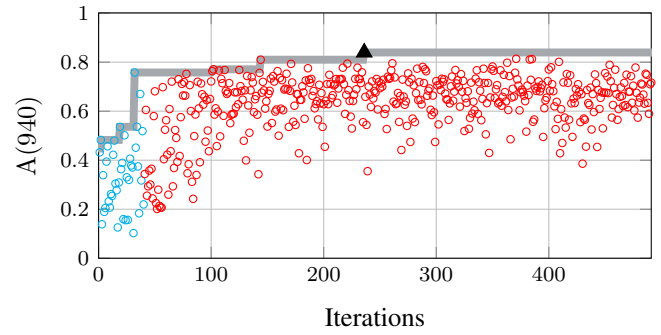

Fig. 8. Objective function as a function of the iterations, for the Bayesian optimization on 3 geometrical parameter, on 2D nanostructured SPAD (see text for details). DOE (resp. EGO) iterations are displayed in blue (resp. red). The maximum reached is 80% and is marked as a black triangle. The grey line is the maximum reached during the optimization.

IV. Conclusion

We demonstrated the relevance of Bayesian global optimization approach with EGO to find optimal geometrical parameters for nanostructured SPAD with DTIs. We ought to mention that optimizing a 2D structure intrinsically limits the scope of the optimum found, since the jump to 3D arises specific difficulties. The first of these difficulties lies in the choice of the grating shapes considered. More 3D grating optimization will be shown at the conference. Moreover, we excluded two structural elements that could be taken into account to optimize a structure closer to the real device: the lens and the non-perfect metal reflector. As a typical example, a lens, by focusing the light inside the SPADs, has a great influence on the grating response, and it should be included in a complete optimization, for instance by varying its radius of curvature.

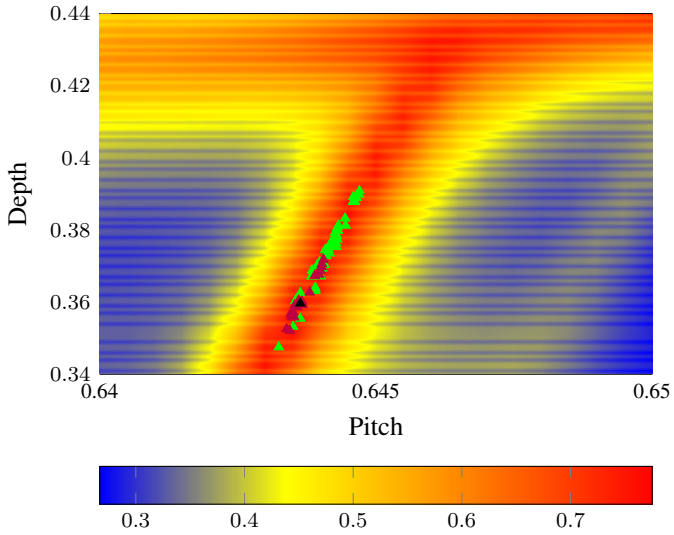

Fig. 9. Linear sweep response, $\mathrm{A}(940)$, on $\left(L_{pitch}, L_{depth}\right)$ and best performing parameters of the EGO optimization. The black triangle marks the optimum reached, purple triangles mark the 20 first best performing parameters. Green triangles mark the 60 best performing parameters (except the first 20, already marked in purple or black). It is worth mentioning that the EGO optimization is able to find the best set of parameters in a few hundreds of iterations, while a linear sweep would require thousands of simulations.

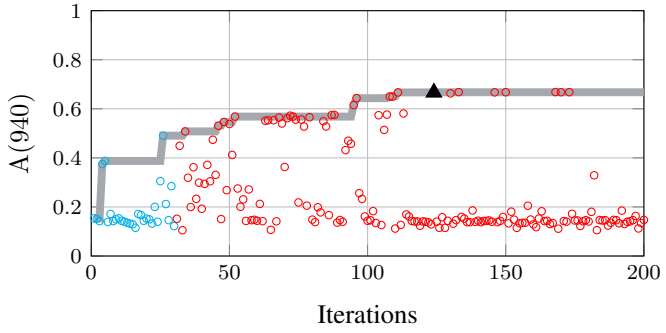

Fig. 10. Objective function as a function of the iterations, for the Bayesian optimization over 2 geometrical parameters, on 3D nanostructured SPAD (see text for details). DOE (resp. EGO) iterations are displayed in blue (resp. red). The maximum reached is 66% and is marked as a black triangle. The grey line is the maximum reached during the optimization.

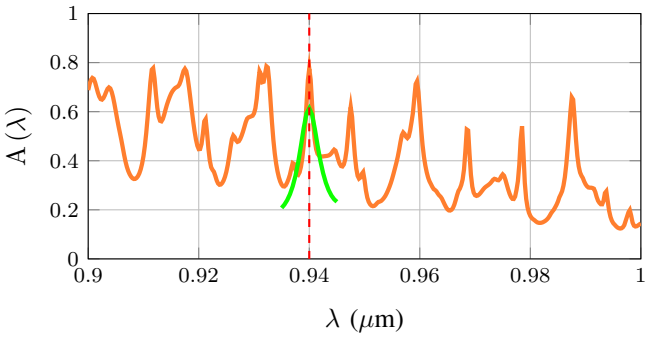

Fig. 11. Absorption profile of the best designs when 2 parameters are optimized on the 3D (green curve) and the 2D (orange curve) nanostructured SPAD. The 3D optimum is obtained with parameters $\left(L_{pitch},\ L_{depth}\right) = (602.8,\ 236.4)$ nm^2. A resonance is positioned exactly at 940 nm. Numerical cost of 3D RCWA simulations allows us to only obtain the absorption profile on a narrow wavelength range around the wavelength of interest.

References

[1] G. Agrawal, *Fiber-Optic Communication Systems: Fourth Edition*, Jan. 2012.

[2] A. Ono, K. Hashimoto, and N. Teranishi, "Near-infrared sensitivity improvement by plasmonic diffraction for a silicon image sensor with deep trench isolation filled with highly reflective metal," *Optics Express*, vol. 29, no. 14, pp. 21 313–21 319, Jul. 2021.

[3] D. Giubertoni, G. Paternoster, F. Acerbi, X. Borrisé, A. Cian, A. Filippi, A. Gola, A. Guerrero, F. P. Murano, F. Romanato, E. Scattolo, and P. Bellutti, "Plasmonic Enhanced Photodetectors for Near Infra-red Light Detection," in *2020 43rd International Convention on Information, Communication and Electronic Technology (MIPRO)*, Sep. 2020.

[4] J. Ma, M. Zhou, Z. Yu, X. Jiang, Y. Huo, K. Zang, J. Zhang, J. S. Harris, G. Jin, Q. Zhang, and J.-W. Pan, "Simulation of a high-efficiency and low-jitter nanostructured silicon single-photon avalanche diode," *Optica*, vol. 2, no. 11, pp. 974–979, Nov. 2015.

[5] Y. Gao, H. Cansizoglu, K. G. Polat, S. Ghandiparsi, A. Kaya, H. H. Mamtaz, A. S. Mayet, Y. Wang, X. Zhang, T. Yamada, E. P. Devine, A. F. Elrefaie, S.-Y. Wang, and M. S. Islam, "Photon-trapping microstructures enable high-speed high-efficiency silicon photodiodes," *Nature Photonics*, vol. 11, no. 5, pp. 301–308, May 2017.

[6] K. Zang, X. Jiang, Y. Huo, X. Ding, M. Morea, X. Chen, C.-Y. Lu, J. Ma, M. Zhou, Z. Xia, Z. Yu, T. I. Kamins, Q. Zhang, and J. S. Harris, "Silicon single-photon avalanche diodes with nano-structured light trapping," *Nature Communications*, vol. 8, no. 1, p. 628, Sep. 2017.

[7] Y. Cao, Z. Zhang, and K. X. Wang, "Photon management with superlattice for image sensor pixels," *AIP Advances*, vol. 11, no. 8, p. 5314, Aug. 2021.

[8] S. Yokogawa, I. Oshiyama, H. Ikeda, Y. Ebiko, T. Hirano, S. Saito, T. Oinoue, Y. Hagimoto, and H. Iwamoto, "IR sensitivity enhancement of CMOS Image Sensor with diffractive light trapping pixels," *Scientific Reports*, vol. 7, no. 1, p. 3832, 2017.

[9] M. M. R. Elsawy, S. Lanteri, R. Duvigneau, J. A. Fan, and P. Genevet, "Numerical Optimization Methods for Metasurfaces," *Laser & Photonics Reviews*, vol. 14, no. 10, p. 1900445, 2020.

[10] E. Garnett and P. Yang, "Light Trapping in Silicon Nanowire Solar Cells," *Nano Letters*, vol. 10, no. 3, pp. 1082–1087, Mar. 2010.

[11] P. I. Frazier, "A tutorial on bayesian optimization," 2018. [Online]. Available: https://arxiv.org/abs/1807.02811

[12] D. M. Whittaker and I. S. Culshaw, "Scattering-matrix treatment of patterned multilayer photonic structures," *Phys. Rev. B*, vol. 60, pp. 2610–2618, Jul 1999.